

# Mg doped Al-rich AlGa<sub>N</sub> alloys for deep UV Emitters

M. L. Nakarmi, K. H. Kim, K. Zhu, J. Y. Lin, and H. X. Jiang<sup>a</sup>

Department of Physics, Kansas State University, Manhattan, Kansas 66506-2601

## ABSTRACT

Mg doped Al-rich AlGa<sub>N</sub> epilayers with Al content as high as 0.7 is needed for obtaining deep UV LEDs with wavelengths shorter than 300 nm. This is one of the most crucial layers in deep UV LEDs and plays an important role for electron blocking and affects the hole injection into the active layer. Not only is this layer critical for the efficiency of deep UV LEDs, it could also introduce long wavelength emission components in UV LEDs. However, it is difficult to obtain high quality Mg doped Al-rich AlGa<sub>N</sub> epilayers and the resistivity of the grown films is usually extremely high. We report here on the growth, optical and electrical properties of Mg doped Al<sub>0.7</sub>Ga<sub>0.3</sub>N epilayers. Mg doped Al<sub>0.7</sub>Ga<sub>0.3</sub>N epilayers of high crystalline and optical qualities have been achieved after optimizing MOCVD growth conditions. Moreover, we have obtained a resistivity around 12,000 Ω cm (near the theoretical limit with Mg doping) at room temperature and confirmed p-type conduction at elevated temperatures for optimized Mg-doped Al<sub>0.7</sub>Ga<sub>0.3</sub>N epilayers. The growth conditions of the optimized epilayer have been incorporated into deep UV LEDs with wavelength shorter than 300 nm. A significant enhancement in power output with a reduction in forward voltage,  $V_f$ , was obtained by employing this optimized Mg doped Al<sub>0.7</sub>Ga<sub>0.3</sub>N epilayer as an electron blocking layer. The long wavelength emission components in deep UV LEDs were also significantly suppressed. The fundamental limit for achieving p-type Al-rich AlGa<sub>N</sub> alloys is also discussed.

**Keywords:** Deep UV LEDs, Al-rich AlGa<sub>N</sub>, Mg doped AlGa<sub>N</sub>

## 1. INTRODUCTION

Al-rich AlGa<sub>N</sub> alloys are ideal materials to realize deep ultraviolet (UV) emitters with wavelength shorter than 300 nm. Chip-scale solid state UV emitters have many applications such as next-generation solid state lighting, fluorescence detection of chemical and biological agents, water purification and medical research [1]. To achieve efficient LEDs in the deep UV range, highly conductive p-type and n-type Al-rich AlGa<sub>N</sub> alloys are needed. It is difficult to grow high crystalline quality AlGa<sub>N</sub> alloys due to large concentration of defects and dislocations in Al-rich AlGa<sub>N</sub> alloys. It is very difficult to achieve highly conductive Al-rich AlGa<sub>N</sub> alloys. With increasing Al content, conductivity decreases mainly due to an increase in the ionization energy of the dopants, alloy scattering and the compensation effect from native defects. In the case of n-type doping, the native defects such as cation vacancies have a dominant effect in compensation. Cation vacancies are acceptor-like defects. The formation energy of cation vacancies in Al-rich AlGa<sub>N</sub> alloys is small and these vacancies are easy to be generated during the growth. But in p-type doping nitrogen vacancies, which are donor-like defects, could be compensating defects as their formation energy is very small [2]. In terms of growth, controlling these defects is necessary to enhance the conductivity by reducing compensation. There has been impressive achievement for n-type conductivity in Al<sub>x</sub>Ga<sub>1-x</sub>N epilayers with Si doping for  $x \geq 0.7$  with resistivity of 0.0075 Ω cm for  $x = 0.7$  [3]. However, it is very difficult to achieve higher p-type conductivity in AlGa<sub>N</sub> due to the large activation energy of the Mg acceptor (160 meV for GaN) in AlGa<sub>N</sub> alloys. P-type conductivity for AlGa<sub>N</sub> is still one of the biggest challenges for the nitride community. We have reported p-type AlGa<sub>N</sub> for Al content up to 27% [4] and Mg doped AlN epilayers [5]. From photoluminescence (PL) results, the Mg level in AlN was found to be 0.5 eV deep from valence band. Mg levels in AlGa<sub>N</sub> become deeper as Al content is increased and it is difficult to obtain sufficient free holes. To enhance the hole carrier concentration, several methods have been explored, such as Mg delta doping [6], short period superlattice (SL) of AlGa<sub>N</sub>/Ga<sub>N</sub> [7] and modulation doped AlGa<sub>N</sub>/Ga<sub>N</sub> SL [8]. Due to the low conductivity of p-type AlGa<sub>N</sub> alloys, injection of holes is still one of the biggest problems in UV LED structure and very low Al content p-AlGa<sub>N</sub> or p-GaN layers have to be used for the hole injection.

For deep UV LED application ( $\lambda < 300$  nm), AlGa<sub>x</sub>N alloy is the unique choice for the active region and cladding layers. Several groups have reported the achievement of deep UV LEDs using AlGa<sub>x</sub>N alloys [9 - 14]. In the UV LED structure, one of the crucial layers is the electron blocking layer. It plays an important role of increasing the density of free electrons in the active region by blocking the injected electron from the n-region thereby enhancing the radiative efficiency. However, it could introduce long wavelength emission components in the UV LEDs when injected electrons overflow to the p-region. These emissions are believed to be related to impurities in AlGa<sub>x</sub>N alloys. Understanding and improving the material quality and conductivity of AlGa<sub>x</sub>N alloys are essential to improve the deep UV LED performance. We report here, the growth, optical and electrical properties of Mg doped Al-rich Al<sub>x</sub>Ga<sub>1-x</sub>N epilayers for  $x \sim 0.7$ . We have achieved Mg doped Al<sub>0.7</sub>Ga<sub>0.3</sub>N epilayers of high crystalline and optical qualities after optimizing the growth conditions. We have achieved p-type conduction at elevated temperature ( $> 700$  K) as confirmed by Hall effect measurement with a resistivity of 40  $\Omega$  cm for optimized Mg doped Al<sub>0.7</sub>Ga<sub>0.3</sub>N epilayer. From the temperature dependence Hall effect measurement, the thermal activation energy of Mg acceptor is estimated to be 320 meV. The optimized growth condition of Mg doped Al<sub>0.7</sub>Ga<sub>0.3</sub>N epilayer was incorporated in the deep UV ( $\lambda < 300$  nm) LED structures in which Mg doped Al<sub>0.7</sub>Ga<sub>0.3</sub>N layer was used as electron blocking layer. The performance of the deep UV LED was significantly improved with an enhancement in output power and a reduction in forward voltage,  $V_f$ . The long wavelength emission components in deep UV LEDs were also significantly suppressed. LEDs of different geometries were fabricated. LEDs with an emission peak wavelength of 292 nm were fabricated with different sized interdigit geometry. With flip chip bonding, an 850  $\mu\text{m} \times 850 \mu\text{m}$  size device has an out put power of 0.74 mW at a 350 mA driving current. The LEDs with 285 nm peak emission wavelengths were fabricated with circular geometry of 275  $\mu\text{m}$  disk diameter. Output power of 0.27 mW was measured at 180 mA current.

## 2. EXPERIMENT

Mg-doped Al<sub>0.7</sub>Ga<sub>0.3</sub>N epilayers of thickness  $\sim 1 \mu\text{m}$  were grown on AlN/sapphire by metalorganic chemical vapor deposition (MOCVD). The AlN epilayer was first grown on sapphire (0001) substrate and followed by Mg doped AlGa<sub>x</sub>N epilayer. The growth of a high quality AlN epilayer prior to the deposition of Mg doped AlGa<sub>x</sub>N epilayers is essential to reduce impurities and dislocation densities. AlN is transparent to deep UV range. AlN also helps for better

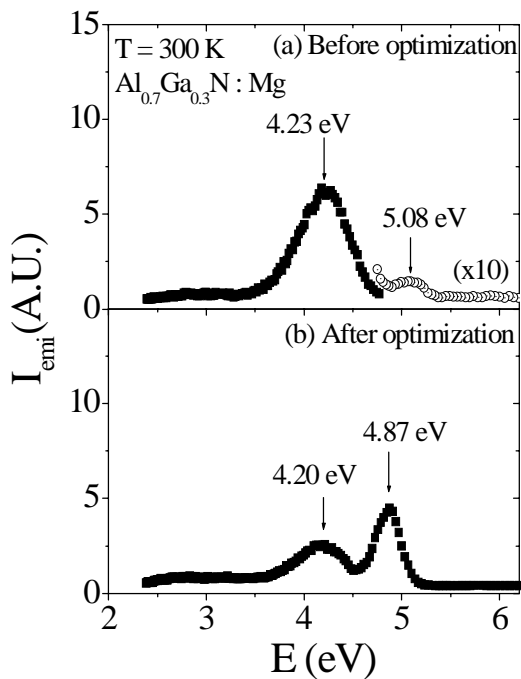


Fig. 1. PL spectra of Mg doped Al<sub>0.7</sub>Ga<sub>0.3</sub>N epilayers measured at room temperature (a) before optimization and (b) after optimization.

heat dissipation as its thermal conductivity is higher than GaN. The benefits of using an AlN epitaxial layer as a template for dislocation density reduction have already been demonstrated [15, 16]. Metal organic sources used were trimethyl aluminum (TMA), trimethylgallium (TMG), and cyclopentadienyl magnesium ( $Cp_2Mg$ ) for Al, Ga, and Mg respectively. Blue ammonia was used for N source. The growth temperature and pressure were 1060°C and 70 torr respectively. The samples were characterized by X-ray diffraction (XRD), deep UV photoluminescence (PL) spectroscopy, and atomic force microscope (AFM). No cracks were found on the samples as revealed by AFM images. XRD was used to determine the aluminum content and crystalline quality. PL spectroscopy was employed to investigate the optical properties of Mg doped  $Al_{0.7}Ga_{0.3}N$  epilayers. The PL system consists of a frequency quadrupled 100 femtosecond Ti:sapphire laser with an average power of 3 mW at 196 nm and repetition rate of 76 MHz. A single photon counting system was employed for time resolved PL measurement to probe the dynamics of the transition. Mg concentration was determined by secondary ion mass spectroscopy (SIMS). The epilayers have a magnesium concentration of about  $1.5 \times 10^{20} \text{ cm}^{-3}$ . As grown epilayers were highly resistive. Post growth rapid thermal annealing in  $N_2$  ambient was done to activate Mg acceptors. Ni/Au was used as contacts in the standard Van der Pauw configuration for Hall effect measurements. Temperature dependence Hall effect measurements were performed with high temperature set up.

The optimized growth condition of Mg doped  $Al_{0.7}Ga_{0.3}N$  epilayer was incorporated in the fabrication of deep UV LED ( $\lambda < 300 \text{ nm}$ ) structures in which Mg doped  $Al_{0.7}Ga_{0.3}N$  layer was used as an electron blocking layer. The LED structure was grown on AlN/sapphire substrate. LEDs of different geometries were fabricated. LEDs with interdigit square geometry of different sizes and different finger numbers were fabricated for LED with 292 nm emission peak. LEDs having 285 nm emission peaks were fabricated with circular geometry of 275  $\mu\text{m}$  diameter. Devices were flip-chip bonded and the power was measured from the sapphire side.

### 3. RESULTS AND DISCUSSION

Figure 1 compares the PL spectra of two typical samples measured at room temperature before and after the optimization of the growth conditions. Resistance and PL spectra were carefully followed to optimize the growth condition. Before optimization, two emission peaks one dominant around 4.2 eV and another small intensity at 5.08 eV,

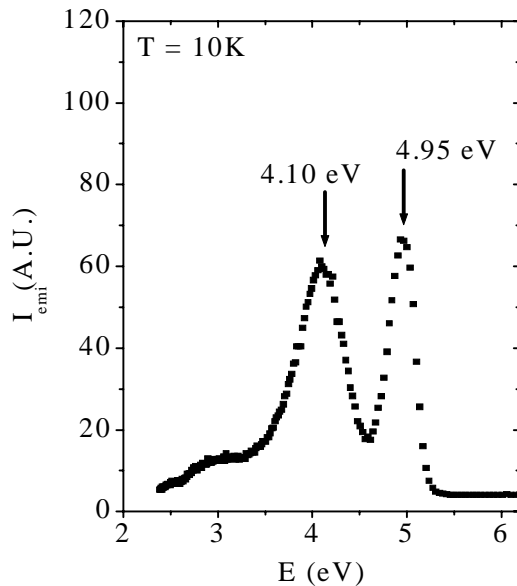


Fig. 2. PL spectra of Mg doped  $Al_{0.7}Ga_{0.3}N$  epilayer at 10 K.

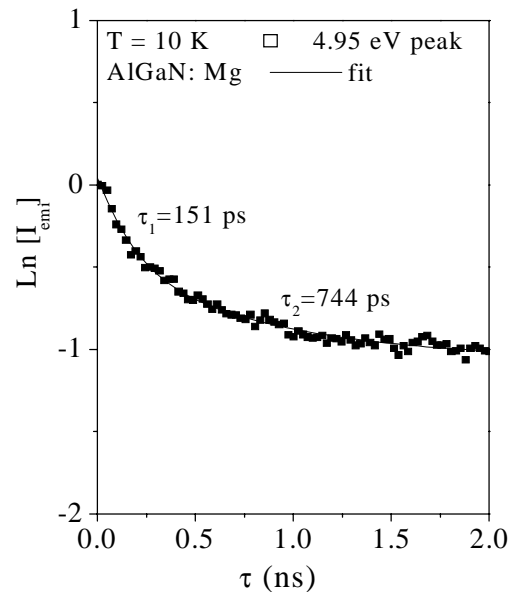


Fig. 3. PL temporal response of the 4.95 eV transition measured at 10 K.

are observed at room temperature. The weak emission at 5.08 eV could be the band-edge transition. The samples with strong impurity transition at 4.2 eV have higher resistances. By optimizing the growth condition (temperature, pressure, V/III ratio, etc), the intensity of the impurity emission at 4.2 eV is suppressed and a strong emission at higher energy peak at 4.87 eV appears as shown in Fig. 1(b). The resistance was then reduced by two orders of magnitude.

Figure 2 shows the PL spectrum of optimized Mg doped  $\text{Al}_{0.7}\text{Ga}_{0.3}\text{N}$  epilayer at 10 K. Fig. 1(b) is the spectrum at room temperature. Two strong emission peaks at 4.95 and 4.10 eV are observed at 10 K. At room temperature peak positions are shifted to 4.87 and 4.20 eV respectively. The emission peak at 4.10 eV has a blue shift at higher temperature as it could be donor-acceptor pair (DAP) type transition. However, the emission peak at 4.95 eV has a red shift indicating the transition is related to band edge. Fig. 3 shows the temporal response of 4.95 eV peak at 10 K. The fitting shows that it has two decay life times of 151 ps and 744 ps. The emission might have two origins. Both of them are in the subnanosecond range indicates that the emissions could be related to conduction band edge. The formation energy of nitrogen vacancy in p-type material is small and it is easy to generate during the growth in Al-rich AlGaN alloys [17]. We believe the peak at 4.2 eV is related to the deep donor of nitrogen vacancy ( $V_N$ ). The emission at 4.2 eV could be due to the transition of electrons from nitrogen vacancy to Mg level and the emission at 4.87 eV could be related to the transition of electrons from conduction band edge to Mg related levels. A strong PL emission intensity at 4.2 eV could be indication of more nitrogen vacancies. Compensation with such donor-like defects decreases the conductivity. Suppressed intensity of the 4.2 eV peak and enhanced intensity of 4.89 eV peak is also correlated with increase in

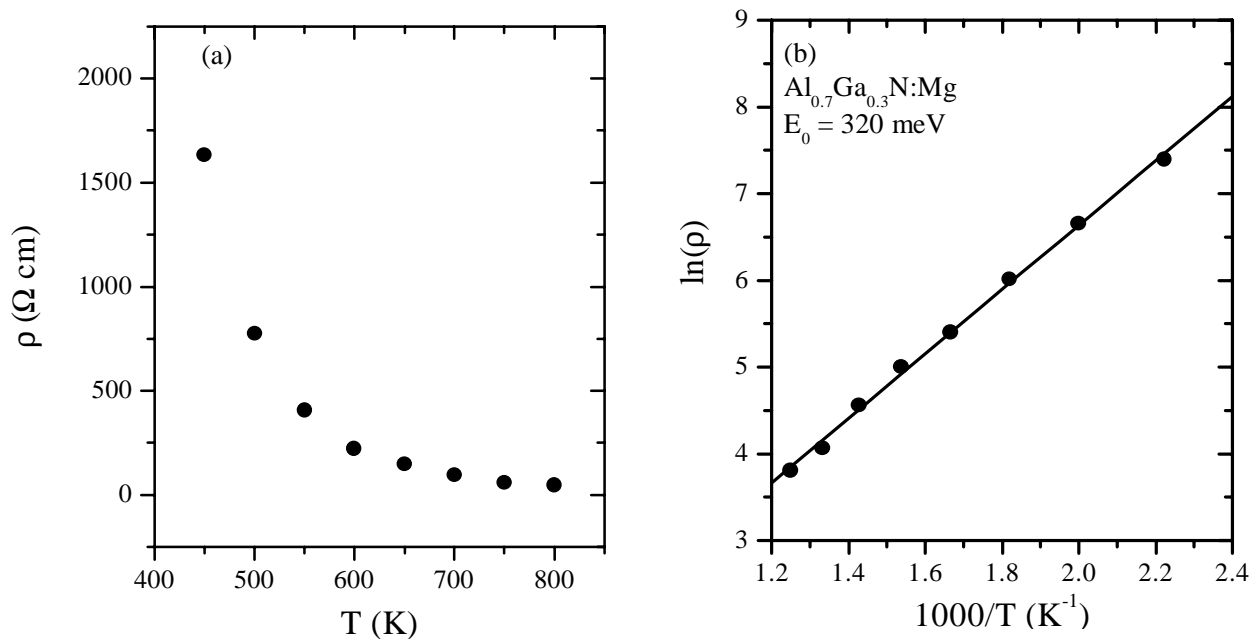


Fig. 4 (a) Variation of resistivity of Mg doped  $\text{Al}_{0.7}\text{Ga}_{0.3}\text{N}$  epilayer in the temperature range 400 to 800 K. (b) From the slope, the activation energy ( $E_0$ ) of Mg acceptor is estimated to be 320 meV.

conductivity of the material. We have found that the growth conditions play an important role in reducing the emission peak around 4.2 eV and enhancing the peak at 4.8 eV.

Fig. 4 shows the results of Hall effect measurement. Fig 4(a) is the variation of resistivity with temperature of a typical sample of Mg doped  $\text{Al}_{0.7}\text{Ga}_{0.3}\text{N}$  epilayer. The resistivity decreases exponentially with increase in temperature. The resistivity decreases about 50 times when the temperature is increased from 450 to 750 K. The smallest resistivity we measured at room temperature is around 12,000  $\Omega$  cm. As the Hall voltage was small, it was difficult to obtain hole concentration. At elevated temperature ( $> 700$  K), it shows p-type signature consistently. At 800 K, the measured

resistivity was about 40  $\Omega$  cm. The mobility was less than 2  $\text{cm}^2/\text{Vs}$ . The activation energy of Mg acceptor was estimated by using the following equation

$$\rho(T) = \rho_0 e^{E_0/kT} \quad (1)$$

where  $\rho(T)$  is the resistivity at temperature  $T$ , and  $E_0$  is the activation energy of acceptor. Fig. 4(b) shows the plot of  $\ln(\rho)$  versus  $1/T$ . From the slope of the linear fit, the activation energy,  $E_0$  is estimated to be 320 meV as shown in Fig. 4(b). This value is lower than our previous estimation of  $E_0$  as a function of the Al content in AlGaN alloys [5]. The thermal activation energy we measured here could be the Mg level with the mobility-edge of free holes, which also decreases  $E_0$ . The Mg level in  $\text{Al}_{0.7}\text{Ga}_{0.3}\text{N}$  alloy could be deeper than 320 meV from valence band. With these values, for the doping concentration of about  $1.5 \times 10^{20} \text{ cm}^{-3}$ , the free hole concentration is in the order of  $10^{14} \text{ cm}^{-3}$  at room temperature.

#### 4. Application in deep UV LED fabrication

The optimized growth condition of Mg doped  $\text{Al}_{0.7}\text{Ga}_{0.3}\text{N}$  epilayer was implemented in the deep UV LED ( $\lambda < 300 \text{ nm}$ ) structure, where Mg doped  $\text{Al}_{0.7}\text{Ga}_{0.3}\text{N}$  layer was used as electron blocking layer. The deep UV LEDs were grown on (0001) sapphire substrates by MOCVD. A high quality epilayer of AlN was first grown as template on sapphire.

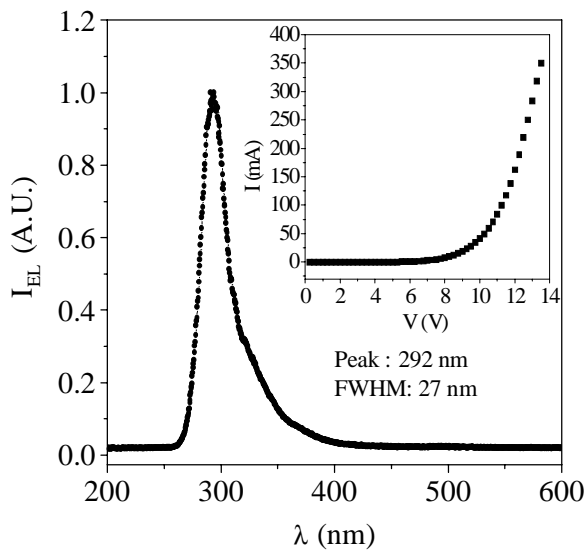


Fig.5. EL spectrum of deep UV LED with a peak at 285 nm under DC bias. Inset: IV characteristic of the LED.  $V_F$  is 9 V at 20 mA current.

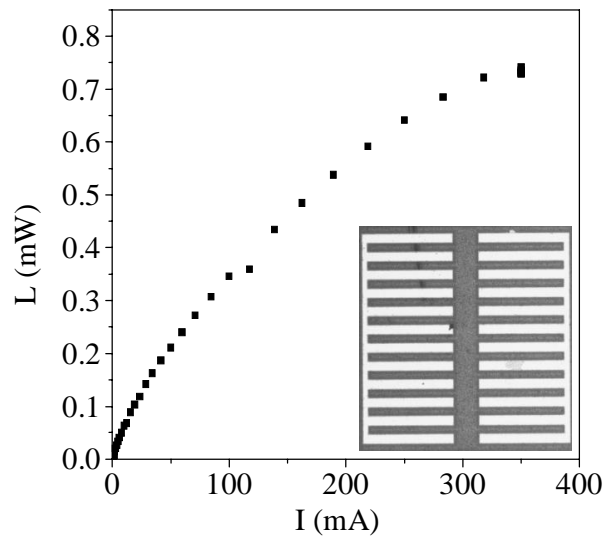


Fig.6. Light output power versus current of 850  $\mu\text{m}$  x 850  $\mu\text{m}$  interdigit LED. Inset: optical microscope image of the fabricated LED

Advantage of using AlN as template is already explained earlier. A highly conductive n- $\text{Al}_{0.7}\text{Ga}_{0.3}\text{N}$  layer of thickness 1.5  $\mu\text{m}$  is then grown on AlN/sapphire template. Subsequent layers are AlGaN based active region followed by Mg doped  $\text{Al}_{0.7}\text{Ga}_{0.3}\text{N}$  electron blocking layer. The structure was completed with p-AlGaN and p-GaN layers. LEDs of different geometry were fabricated. The fabrication started from the deposition of a Ni/Au transparent layer and mesa etching to expose the n- $\text{Al}_{0.7}\text{Ga}_{0.3}\text{N}$  followed by Ti/Al metal deposition for the n-contact and Ni/Au for p-contact with rapid thermal annealing at 650 $^\circ\text{C}$  for 2 min. Devices with different geometry were then diced into single devices, flip-

chip bonded with Au bumps onto ceramic AlN submount and finally mounted on TO headers. Deep UV LEDs with a peak emission at 292 nm were fabricated with interdigit square geometry. Fig. 5 shows the electroluminescence (EL) of the deep UV LED with peak at 292 nm. It has FWHM of 27 nm at 40 mA DC driving current. Inset of Fig. 5 shows I-V characteristics of the LED. It has forward voltage,  $V_f$  of 9 V at 20 mA current. Fig. 6 shows L-I characteristic of the LED. Inset of Fig. 6 shows the optical microscope image of a 12 fingers interdigit device. The maximum power measured for a device with 12 fingers is 0.74 mW at a driving current of 350 mA. We also have LEDs with peak emission at 285 nm, which were fabricated with circular geometry of 275  $\mu\text{m}$  diameter [18]. The maximum power reached to 0.27 mW with a power density of 0.45  $\text{W}/\text{cm}^2$  at 180 mA current. The life time of these LEDs are observed  $> 1000$  hours. We have observed that with incorporation of the optimized growth condition of Mg doped  $\text{Al}_{0.7}\text{Ga}_{0.3}\text{N}$  epilayer in the blocking layer, we could enhance the output power. The long wavelength shoulder was dramatically reduced along with forward voltage,  $V_f$ . Further improvement of the conductivity of Mg doped AlGa $\text{N}$  epilayer is required to enhance the efficiency and performance of deep UV LEDs, especially when shorter wavelength emission is required.

## 5. SUMMARY

In summary, we have grown high quality Mg doped  $\text{Al}_{0.7}\text{Ga}_{0.3}\text{N}$  epilayers by MOCVD. Optical and electrical properties of the epilayers were studied. From PL results, we found a dominant emission peak at 4.2 eV, which is a signature of higher resistivity of the material in Mg doped  $\text{Al}_{0.7}\text{Ga}_{0.3}\text{N}$  epilayers. Suppressed PL intensity at 4.2 eV and enhanced intensity at 4.8 eV correlate with the improved conductivity. At room temperature, we measured a resistivity around 12000  $\Omega$  cm. We have obtained p-type resistivity of about 40  $\Omega$  cm at 800 K. The thermal activation energy of Mg is estimated to be 320 meV for Mg doped  $\text{Al}_{0.7}\text{Ga}_{0.3}\text{N}$  epilayer from temperature dependence resistivity measurement. The optimized growth condition of the epilayer was incorporated in the fabrication of deep UV LED ( $< 300$  nm) in which Mg doped  $\text{Al}_{0.7}\text{Ga}_{0.3}\text{N}$  layer was used as an electron blocking layer. There was a significant improvement of LED performance in terms of power output, forward voltage and emission spectrum. LEDs of interdigit geometry were fabricated for LEDs having an emission peak at 292 nm. A maximum power of 0.74 mW was measured at 350 mA driving current. LEDs of circular geometry of 275  $\mu\text{m}$  disk diameter were fabricated for LEDs having peak emission wavelength at 285 nm. The output power reached 0.27 mW with a power density of 0.45  $\text{W}/\text{cm}^2$  at driving current of 180 mA.

This work is supported by the grants from DARPA, ARO, NSF, and DOE.

### References:

(a) Email: jiang@phys.ksu.edu

- [1] A. Bergh, G. Craford, A. Duggal, and R. Haitz, *Physics Today*, **December** 2001, page 42.
- [2] C. G. Van de Walle and J. Neugebauer, *J. Appl. Phys.* **95**, 3851 (2004).
- [3] M. L. Nakarmi, K. H. Kim, K. Zhu, J. Y. Lin and H. X. Jiang, submitted to *Appl. Phys. Lett.*
- [4] J. Li, T. N. Oder, M. L. Nakarmi, J. Y. Lin, and H. X. Jiang. *Appl. Phys. Lett.* **80**, 1210 (2002).
- [5] K. B. Nam, M. L. Nakarmi, J. Li, J. Y. Lin, and H. X. Jiang. *Appl. Phys. Lett.* **83**, 878 (2003).
- [6] M. L. Nakarmi, K. H. Kim, J. Li, J. Y. Lin, and H. X. Jiang. *Appl. Phys. Lett.* **82**, 3041 (2003).
- [7] A. Saxler and W. C. Mitchel, P. Kung and M. Razeghi, *Appl. Phys. Lett.* **74**, 2023 (1999).
- [8] E. L. Waldron, J. W. Graff, and E. F. Schubert, *Appl. Phys. Lett.* **79**, 2737 (2001).
- [9] V. Adivarahan, S. Wu, J. P. Zhang, A. Chitnis, M. Shatalov, and V. Mandavilli, R. Gaska and M. Asif Khan. *Appl. Phys. Lett.* **84**, 4762 (2004).
- [10] J. P. Zhang, A. Chitnis, V. Adivarahan, S. Wu, V. Mandavilli, R. Pachipulusu, M. Shatalov, G. Simin, J. W. Yang, and M. Asif Khan, *Appl. Phys. Lett.* **81**, 4910 (2002).
- [11] A. Yasan, R. McClintock, K. Mayes, D. Shiell, L. Gautero, S. R. Darvish, P. Kung, and M. Razeghi, *Appl. Phys. Lett.* **83**, 4701 (2003).
- [12] A. Hanlon, P. M. Pattison, J. F. Kaeding, R. Sharma, P. Fini, and S. Nakamura, *Jpn. J. Appl. Phys., Part 2* **42**, L628 (2003).
- [13] A. J. Fischer, A. A. Allerman, M. H. Crawford, K. H. A. Bogart, S. R. Lee, R. J. Kaplar, W. W. Chow, S. R. Kurtz, K. W. Fuller, and J. J. Figiel, *Appl. Phys. Lett.* **84**, 3394 (2004).

- [14] S. Wu, V. Adivarahan, M. Shatalov, A. Chitnis, W. Sun, and M. Asif Khan. *Jpn. J. Appl. Phys.* **43**, L1035 (2004).
- [15] S. Arulkumaran, M. Sakai, T. Egawa, H. Ishikawa, and T. Jimbo, T. Shibata, K. Asai, S. Sumiya, Y. Kuraoka, M. Tanaka, and O. Oda, *Appl. Phys. Lett.* **81**, 1131 (2002).
- [16] B. Zhang, T. Egawa, H. Ishikawa, Y. Liu, and T. Jimbo, *J. Appl. Phys.* **95**, 3170 (2004).
- [17] C. Stampfl and C. G. Van de Walle. *Phys. Rev. B* **65**,155212 (2002).
- [18] K. H. Kim, Z. Y. Fan, M. Khizar, M. L. Nakarmi, J. Y. Lin, and H. X. Jiang. submitted to *Appl. Phys. Lett.*